Effects of Antiagglomerants on the Interactions between Hydrate Particles

Mark R. Anklam
Dept. of Chemical Engineering, Rose-Hulman Institute of Technology, Terre Haute, IN 47803

J. Dalton York
Dept. of Chemical Engineering, Yale University, New Haven, CT, 06520

Luke Helmerich
Dept. of Chemical Engineering, Rose-Hulman Institute of Technology, Terre Haute, IN 47803

Abbas Firoozabadi
Reservoir Engineering Research Institute, Palo Alto, CA 94306

DOI 10.1002/aic.11378
Published online December 27, 2007 in Wiley InterScience (www.interscience.wiley.com).

Hydrate inhibition in natural gas production by antiagglomeration is promising because of effectiveness at high subcoolings encountered in many offshore operations. There are various mechanisms that are believed to contribute to the repulsion and attraction of hydrate particles. These include: (1) steric, (2) dispersion, (3) capillary, and (4) shear forces. Some of the expressions derived, and some formulas are used from the literature to provide a theoretical analysis of the forces between two hydrate particles to examine antiagglomeration using surfactants. Results show that hydrate particle size has the most important effect on antiagglomeration. Results also show that the contact angle increase and the oil-water interfacial tension decrease will either reduce capillary forces significantly or eliminate it. Effective antiagglomerants reduce the size, decrease interfacial tension, and increase contact angle through the water phase. © 2007 American Institute of Chemical Engineers *AIChE J,* 54: 565–574, 2008
Keywords: gas hydrates, antiagglomeration, capillary force, steric repulsion, natural gas production

Introduction

The undesirable formation of gas hydrates in natural gas pipelines, and their prevention is a problem that has received considerable interest. In subsea pipelines, the presence of water combined with low-temperatures and high-pressures provides conditions that are favorable for the formation of hydrates. These crystalline compounds can agglomerate and form plugs in the pipelines. The costs associated with production loss and plug removal can be substantial. Traditionally, large quantities (15–50% of the free water) of a thermodynamic inhibitor (e.g., methanol or ethylene glycol) are added to shift equilibrium conditions, such that hydrate formation is no longer thermodynamically favorable. The large quantities of added chemicals present both economic and environmental concerns. Much research has been conducted to identify and develop low-dosage hydrate inhibitors (LDHI) that may be used at lower concentrations, and that affect the interfacial properties of a hydrate-forming system rather than the bulk phase properties as do thermodynamic inhibitors. LDHI interact with the hydrate surface to prevent[1]

A. Firoozabadi is also affiliated with the Dept. of Chemical Engineering, Yale University, New Haven, CT 06520.
Correspondence concerning this article should be addressed to A. Firoozabadi at abbas.firoozabadi@yale.edu.

or slow the formation of hydrate plugs. There are two types of LDHI that act by very different mechanisms. Kinetic inhibitors (KI) adsorb onto growing hydrate crystals at the hydrate/water interface to slow the rate of growth; they may also slow the rate of nucleation of hydrate crystals. Antiagglomerants (AA) disperse the hydrate particles in oil that is present and keep the particles from adhering together. AA generally do not affect the rate of formation of hydrates. They prevent the particles from agglomerating and forming a plug, and appear to hold the most promise because of effectiveness at the large subcoolings experienced in subsea pipelines and for prolonged shutins when pipline flow is stopped.

Despite the promise of AA, many aspects of the fundamental mechanisms by which hydrate particles agglomerate and form blockages, and by which AA are effective have remained unclear. The focus of this work is on the examination of the mechanisms of hydrate agglomeration and of the effects of surface-active additives on antiagglomeration.

Particle adhesion

To understand the mechanism by which AA act, one must first understand how hydrate particles adhere to each other. There are two main types of forces acting to hold the particles together—dispersion forces (London—van der Waals) and capillary forces. The dispersion forces depend primarily on the particle size, the particle composition, the composition of the medium, and the distance between particles. Capillary forces are present when a liquid bridge connects two particles. These forces will depend on the particle size, the interfacial tension between the bridging liquid (water), and the liquid in which the particles are dispersed (oil), the contact angle at the particle surface, the distance between particles, and the volume of bridging liquid.

For gas hydrates, Lund and Larsen[2] have observed that lowering temperature leads to reduced particle adhesion, and have developed a cold flow approach to preventing hydrate blockage. They observed that during cooling and hydrate formation, hydrates go from a slushy stage, to a sticky stage (where particles adhere to each other readily) to a nonaggregating particulate stage. Lund and Larsen (and others[3]) have investigated the use of flow loops to create these "dry" particles in a controlled way rather than allow for "sticky" particles in the flow lines. Adhesion studies on hydrate and ice particles show the same effect where particle adhesion decreases as the subcooling (the difference between hydrate melting or dissociation temperature and system temperature) increases.[4–6]

It has been suggested that dispersion forces between separated spheres would not be strong enough to describe the attractive force that causes aggregation, and that solid-solid adhesion forces (dispersion forces for deformed spheres in contact accounted for in models, such as Derjaguin-Muller-Toporov (DMT)[7] or Johnson-Kendall-Roberts (JKR)[8] theories), present at particle contact, cannot explain the temperature effects.[4,5] The strong adhesion and the temperature effects are believed to be due to capillary forces, which also can describe forces measured in rheological studies and particle interaction studies.[2,4–6,9]

Antiagglomeration

AA are surface-active molecules which are hydrophobic, and adsorb at the water-oil and hydrate-oil interfaces, and disperse the water as droplets and stabilize the particles against permanent adhesion. Both water and oil (or condensate liquid) are naturally present in the wellstream. In some cases surface-active molecules are also naturally present in the oil (not in the natural gas), but usually they are added to the system to prevent agglomeration. In the following, the term "surfactant" will be used in a general sense and could refer to a polymer, a naturally occurring AA, or a traditional surfactant. Kelland[10] has an extensive review of AA and KI development with many examples of molecules that have been studied as AA.

Surfactants are frequently used to alter particle adhesive properties; however, there are many mechanisms by which the surfactants can affect interfacial forces.[11,12] The main mechanism by which AA are thought to work is by introducing steric repulsion between adsorbed surfactants on the hydrate particles in order to prevent contact.[13] However, if capillary forces are a primary cause of agglomeration, AA must also reduce or eliminate capillarity through adsorption. Surfactants may also provide repulsion through electrostatic and structural forces; these forces may not contribute significantly in hydrates for AA. In addition to affecting the forces between particles, AA may affect the dispersion of the hydrate particles by adsorbing on the hydrate surface.[10,14]

The purpose of this article is to examine the forces in agglomeration and stabilization of hydrate particles and the effects of AA adsorption at interfaces. In this work, we will first present theory behind repulsive forces (steric forces) and attractive forces (dispersion and capillary forces), to provide a quantitative analysis of the mechanism by which AA act. We will also briefly examine simple shear forces to determine the degree to which overall adhesive forces need to be reduced for flow to separate particles. Then we will present results from the theory to illustrate how AA may influence the interaction between particles followed by a discussion on the effects of AA adsorption and wettability. At the end we will draw a few conclusions. In this paper, we will not examine the chemistry of various AA or the mechanism of AA adsorption as has been examined by others.[10,13–15]

Theory

Steric forces

When adsorbed layers of surfactant or polymer on particle surfaces come into contact, the interactions between the chains can lead to a net repulsion between particles. By preventing contact between hydrate particles, the strong adhesive forces (solid-solid adhesion and capillary adhesion) may be reduced or prevented.

A full, quantitative model may be developed to describe the interactions. However, the system is very complex and involves not only interactions between chains, but also equilibrium adsorption effects. Fleer et al.[16] describe some in-depth modeling of polymer adsorption and interactions. Simple models of chain overlap and the balance of repulsive and attractive forces can also be used to highlight the effects of important parameters and estimate the magnitude of repulsive forces (or energies) relative to attractive ones. These models can give estimates of interaction energies or forces for small overlap distances, but they would be expected to become less accurate as the degree of overlap increases.

One theory is based on the superposition of chains in the region of overlap. The concentration of chains in this region

is assumed to be twice the concentration in the adsorbed layers where the concentration of chains is constant. Any chain rearrangement effect on adsorption is neglected. The free energy change for repulsion (or the potential between two spheres ϕ_s) from chain overlap is given by[17]

$$\Delta G = \Phi_s = \Delta G_{m,2\phi_2} - 2\Delta G_{m,\phi_2} \tag{1}$$

where ΔG_m is the Gibbs free energy of mixing, and ϕ_2 is the volume fraction of surfactant chain in the adsorbed layer (assumed to be uniform), which doubles in the overlap region. Without overlap, $\Delta G = 0$. The free energy change in the layers is calculated from Flory-Huggins theory, and for two spheres of radius a, the change in free energy due to overlap (or the potential ϕ_s) is given by[16–18]

$$\Delta G = \Phi_s = \frac{4\pi kT\phi_2^2}{3v_1}(1/2 - \chi_{12})(\delta - h/2)^2(3a + 2\delta + h/2); \quad h \le 2\delta \tag{2}$$

where all terms greater than second order in ϕ_2 are neglected, and where v_1 is the molecular volume of solvent (the volume of a lattice site), k is Boltzmann's constant, T is temperature, χ_{12} is the Flory-Huggins interaction parameter, δ is the thickness of the adsorbed layer, and h is the closest distance between particles. Neglecting any free polymer/surfactant in the adsorbed layer, the surface concentration (molecules per area) of adsorbed material is given by

$$\Gamma = \frac{\phi_2\delta}{rv_2} \tag{3}$$

where v_2 is the volume per repeat unit of the chain, and r is the number of repeat units in the adsorbed molecule. The repulsive force can be found from

$$F_s = -\frac{\partial\Phi_s}{\partial h} = \frac{4\pi akT\phi_2^2}{v_1}(1/2 - \chi_{12})(\delta - h/2) \tag{4}$$

with the assumption that $a >> \delta$.

An alternative theory for the Gibbs free energy change of repulsion has been suggested by Everett.[18,19] In this theory, the change in free energy is computed for two parallel plates with adsorbed polymer or surfactant as a function of the distance (see Appendix). We derive, using the Derjaguin approximation,[20] the repulsive potential between spheres

$$\Phi_s = \pi akT\left[\begin{array}{l} 4\Gamma^2 v_2 r^2\left(\ln\left(\frac{2\delta}{h}\right) - \frac{2\delta - h}{2\delta}\right)(1/2 - \chi_{12}) \\ + (8/3)\Gamma^3 r^3 v_2^2\chi_{12}\left(\frac{1}{h} - \frac{1}{2\delta} - \frac{2\delta - h}{4\delta^2}\right) \end{array}\right]; \quad h \le 2\delta \tag{5}$$

The repulsive force is then derived to be

$$F_s = \pi akT\left[4\Gamma^2 v_2 r^2\left(\frac{1}{h} - \frac{1}{2\delta}\right)(1/2 - \chi_{12}) + (8/3)\Gamma^3 r^3 v_2^2\chi_{12}\left(\frac{1}{h^2} - \frac{1}{4\delta^2}\right)\right] \tag{6}$$

The expressions in Eqs. 2 and 5, and those in Eqs. 4 and 6 are different in form, but interestingly they show the same basic trend at small overlap distances. We will use the superposition model in later analyses except when we compute the potential between two particles for the combined effect of thermodynamic inhibitors and AA.

As can be seen from Eqs. 2 and 5, the interaction energy is strongly dependent not only on the layer thickness and distance of separation, but also on the concentration of adsorbed material and interaction of solvent and stabilizing chain. In a good solvent, chain segments favor contact with the solvent and $\chi_{12} < 0.5$. The quality of solvent improves with a decrease in χ_{12}, and the interaction energy becomes more positive (repulsive) as Eq. 2 indicates. The interaction between solvent and stabilizing molecule may also have a large effect on the amount of adsorbed material. Thus, variations in solvent composition from the presence of thermodynamic inhibitors such as methanol may affect the repulsion.

To study the effect of both AA and thermodynamic inhibitors, one would need to account for the presence of the second solvent in the free energy of mixing using a modified Flory-Huggins theory[21,22]

$$\Delta G_m = kT\left(\begin{array}{l} n_1\ln\phi_1 + n_2\ln\phi_2 + n_3\ln\phi_3 + \chi_{12}n_1\phi_2 \\ + \chi_{13}n_1\phi_3 + \chi_{23}n_2\phi_3 + \chi_T n_1\phi_2\phi_3 \end{array}\right) \tag{7}$$

where n_i are the molecules of species i (1 and 2 are the solvents, and 3 is the surfactant segment), ϕ_i are the volume fractions of species i, χ_{ij} are the interaction parameters between species i and j, and χ_T is the ternary interaction parameter. The ternary interaction parameter accounts for anisotropic interactions (deviations from Flory-Huggins theory); it typically appears as a correction factor, and in some cases good agreement between theory and data is found only by including the ternary interaction term.[22] In this work, we assume that the ternary interaction parameter can be neglected.

Equation 7 can be used with the superposition method for the two spheres (Eq. 1). Combining Eq. 7 with Eq. 1 (taking as a reference state the premixed solvents), while neglecting any terms higher than second-order in ϕ_3, and using the volume of the overlap region gives an equation similar in form to Eq. 2

$$\Phi_s = \frac{4\pi kT\phi_3^2}{3v_1}\left(1/2 - \frac{\chi_{13}}{1+m} - \frac{\chi_{23}m}{1+m} + \frac{\chi_{12}m}{(1+m)^2}\right) \times (\delta - h/2)^2(3a + 2\delta + h/2) \tag{8}$$

where m is the ratio of solvent 2 to solvent 1; $m = \phi_2/\phi_1$. Using the method of Everett rather than superposition (see Appendix), the force between spheres is found to be

$$F_s = \pi akT\left[\begin{array}{l} 4\Gamma^2 r^2 v_3\left(\frac{1}{h} - \frac{1}{2\delta}\right)\left(\frac{1}{2} - \frac{\chi_{13}}{1+m} - \frac{\chi_{23}m}{1+m} + \frac{\chi_{12}m}{(1+m)^2}\right) \\ + (8/3)\Gamma^3 r^3 v_3^4\left(\frac{1}{h^2} - \frac{1}{4\delta^2}\right)\left(\frac{\chi_{13}}{1+m} + \frac{\chi_{23}m}{1+m} - \frac{\chi_{12}m}{(1+m)^2}\right) \end{array}\right] \tag{9}$$

For hydrocarbon stabilizing chains in an aliphatic hydrocarbon solvent (1), with an alcohol (2), χ_{23} and χ_{12} may have quite comparable values, and Eqs. 8 and 9 would predict only a small effect assuming that Γ remains constant. The second solvent is also likely to affect interfacial properties and the size of water droplets dispersed in the oil (and, thus, the size of the particles).

The main issue relating to hydrate particle stability is how the surfactant affects the total interaction energy and not just the repulsive interaction energy. As it will be seen, sometimes even large changes in the repulsive force have little effect on the net attractive force holding particles together.

Next the expression for attractive potential between spheres due to dispersion forces will be presented.

Dispersion forces

The attractive potential due to dispersion forces between two spheres of radius a separated by h is given by[23]

$$\Phi_s = -\frac{1}{6}A\left[\frac{2a^2}{4ah+h^2}+\frac{2a^2}{4a^2+4ah+h^2} + \ln\left(\frac{4ah+h^2}{4a^2+4ah+h^2}\right)\right] \quad (10)$$

where A is the Hamaker constant. The force between spheres can be found from Eq. 10

$$F_s = \frac{aA}{12h^2} \quad (11)$$

where we have assumed that $a \gg h$. As an estimate it can be assumed that the attractive potential from dispersion forces, and the repulsive potential from steric forces are additive, and that the presence of the hydrocarbon stabilizing chain will not affect the behavior of the hydrocarbon medium (i.e., the Hamaker constant will not vary with h). A is estimated to be about 5×10^{-21} J for hydrates in oil,[9] and for the purposes of illustration retardation effects (a decrease in A with increasing h) will be ignored. Solid-solid adhesion theories such as DMT and JKR are not examined in this article, because the focus of analysis will be on particles separated by a steric layer and not in contact.

Capillary forces

Liquid water, from either a liquid-like layer on the surface of the hydrate (as found on ice), or from water outside of the hydrate particles, can bridge two hydrate particles and give rise to an attractive force.[4] The idea behind this proposed mechanism in the absence of free liquid water is capillary condensation.[24–27] Liquid water can form a liquid bridge at the contact point between hydrate particles (as shown in Figure 1) when the curvature of the oil/water interface is high-enough (if the water preferentially wets the hydrate particle). Then the reduced pressure of the liquid water due to the curved interface (compared to pressure of the hydrate particle) could cause the chemical potential of water to be lowered to the point where liquid water is thermodynamically stable, and at equilibrium with the water in the hydrate. This reduced pressure in the liquid neck compared with the oil pressure gives rise to an increase in attractive force between hydrate particles. A simple

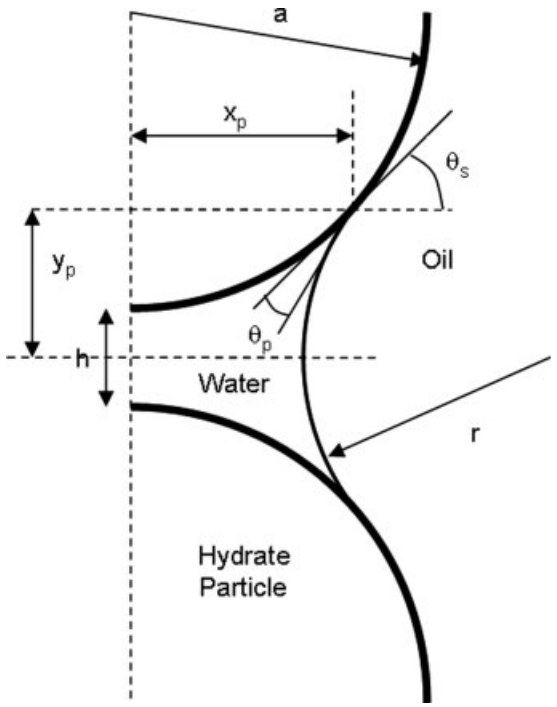

Figure 1. Liquid water bridge connecting two spherical hydrate particles dispersed in oil.

estimate of this attractive force between two spheres of radius a at contact is given by[24]

$$\frac{F_s}{a} = 2\pi\sigma\cos\theta_p \quad (12)$$

where σ is the interfacial tension between the water and the oil, and θ_p is the contact angle of the water on the hydrate particle.

To model the effects of capillary forces on hydrate particle adhesion, hydrate particles will be modeled as spheres. Figure 1 shows a liquid bridge connecting two spherical particles separated by a distance h. Eq. 12 gives an estimate of the attractive force due to capillary adhesion based on the assumption of perfect spheres at contact. The expression for the force between two spheres separated by distance h can be derived following the work of de Lazzer et al.[28] (these authors provide an expression for the force between a sphere and plate). We assume the cross-section of the liquid/liquid interface (between the water bridge and the surrounding oil) to be circular and derive the following expression for the attractive force (positive if attractive)

$$F_s = -\pi x_p^2\sigma\left(\frac{1}{x_p}-\frac{1}{r}\right) + 2\pi x_p\sigma\sin\left(\theta_p+\theta_s\right) \quad (13)$$

where x_p, r, θ_p, and θ_s are defined in Figure 1, and σ is the interfacial tension between the oil and water (as defined before). The first term on the righthand side in Eq. 13 gives the force arising from the capillary pressure across the curved interface (a lowered pressure between particles), and the second is from the interfacial tension forces acting tangentially to the interface along the contact line which is

usually small except at large x_p. The radii of curvature, x_p and r, are related by

$$r = \frac{(h/2) + 1 - \left(a^2 - x_p^2\right)^{1/2}}{\cos\left(\theta_p + \theta_s\right)} \tag{14}$$

with

$$\theta_s = \arctan\left(\frac{x_p}{\left(a^2 - x_p^2\right)^{1/2}}\right) \tag{15}$$

Then from Eqs. 13 to 15, the attractive force can be calculated for any x_p given a, h, θ_p, and σ.

For a stable liquid water bridge connecting hydrate (or ice) particles, the chemical potential of the liquid water must be the same as that of the water in the particle. This means that for any subcooling ($T_m - T$), where T_m is the melting point temperature or dissociation temperature), x_p and r will be fixed for a given h. For a single component system (ice) the equilibrium relationship is given approximately by

$$\sigma\left(\frac{1}{x_p} - \frac{1}{r}\right) = -\frac{L\Delta T}{T_m \overline{V}} \tag{16}$$

where L is the latent heat, and $\overline{V}$ is the molar volume of water. For hydrates, L should be replaced by ΔH_w, the change in enthalpy of water between the two phases.

We mentioned in the Introduction that adhesion forces between hydrate particles have been measured to increase as subcooling decreases.[4–6] As Eq. 16 shows, temperature affects curvature. The temperature may also affect the attractive force through a change in both σ and θ_p (which is a function of both σ, and the solid surface energies). These latter effects are not accounted for in the results presented later.

Shear forces

As Figure 2 shows, the net attractive potential between very small particles may be quite small ($<kT$), such that Brownian motion could allow separation. For particles larger than 100 nm in radius, the attractive potential would be greater than $2kT$ for the case of particles stabilized with C_{16} chains (see Results section). However, the forces experienced during flow may be enough to break apart the flocs.

The shear force necessary to separate a pair of particles can be estimated assuming simple shear flow. The shear force in this case would be[23]

$$F_{\text{shear}} = 6\pi\mu a^2\gamma \tag{17}$$

where γ is the shear rate, and μ is the viscosity. For a pair of particles being held by dispersion forces (Eq. 11), the particle size necessary for forces to balance is given by

$$a = \frac{A}{72\pi h^2 \mu\gamma} \tag{18}$$

In the Results and Discussion section these equations will be used to compare with the magnitude of capillary, and dispersion forces to see if irreversible aggregation (agglomeration) would be expected.

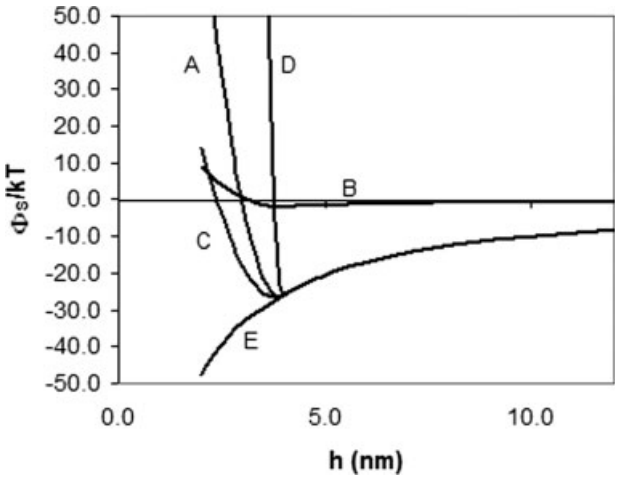

Figure 2. Net potential between spheres using Eqs. 2 and 10.

Curve A: $a = 1$ μm, $\chi_{12} = 0.3$, $\Gamma = 5 \times 10^{17}$ molecules/m^2; B: $a = 100$ nm, $\chi_{12} = 0.3$, $\Gamma = 5 \times 10^{17}$ molecules/m^2; C: $a = 1$ μm, $\chi_{12} = 0.4$, $\Gamma = 5 \times 10^{17}$ molecules/m^2; D: $a = 1$ μm, $\chi_{12} = 0.3$, $\Gamma = 2 \times 10^{18}$ molecules/m^2; E: $a = 1$ μm, $\chi_{12} = 0.3$, $\Gamma = 1 \times 10^{17}$ molecules/m^2. Other parameters are given in the text.

Results and Discussion

Combined effects of steric and dispersion forces

Figure 2 shows a comparison of the effects of various parameters on the net potential from adding Eqs. 2 and 10. The parameters used in the plots are $v_1 = 2.7 \times 10^{-28}$ m^3 (approximately the molecular volume of octane), $v_2 = 6 \times 10^{-29}$ m^3 (approximately the volume of an ethylene mer), $\delta = 2$ nm (about the distance of a fully extended C_{16} chain), $r = 8$ (repeat units in the C_{16} chain). As a reference condition (curve A) we choose $a = 1$ μm, $\chi_{12} = 0.3$ (conservative estimate for the value for polyethylene in octane), and $\Gamma = 5 \times 10^{17}$ molecules/m^2. Curve B shows the effect of particle size with $a = 100$ nm. Curve C shows the effect of solvent quality with $\chi_{12} = 0.4$. Curves D and E show the effects of surface concentration with $\Gamma = 2 \times 10^{18}$ molecules/m^2 for D and $\Gamma = 1 \times 10^{17}$ molecules/m^2 for E. Potential is approximately proportional to particle size, so an order of magnitude change in particle size gives rise to about an order of magnitude change in the attractive minimum potential as seen from curves A and B. The system with $a = 100$ nm has an attractive minimum of approximately $-2kT$ (a relatively weak attraction), while the system with $a = 1$ μm has an attractive minimum of approximately $-26kT$ (a strong attraction). However, the increase in adsorption concentration (curve D), and the decrease in solvent quality (curve C) have a significant effect on the repulsive potential and repulsive force in the stabilizing layer, but they do not significantly affect the attractive minimum potential or the maximum attractive force between particles (smallest value of dF_s/dh). The effects of surface concentration and solvent quality on δ are neglected (it is assumed that the chains are always fully extended). The main point is that as long as there is a sufficient amount of adsorbed material, additional amounts of adsorbed material or relatively small changes in solvent

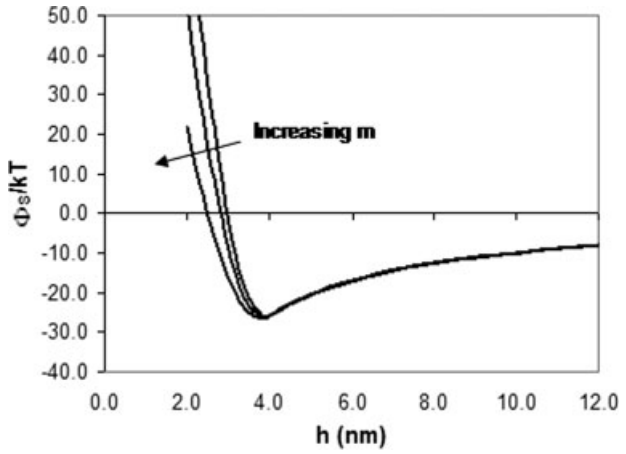

Figure 3. Net potential between spheres using Eqs. 8 and 10 to show the effects of a binary solvent with *m* increasing from 0 to 0.1 to 0.2.

$\chi_{13} = 0.3$, $\chi_{12} = 0.8$, and $\chi_{23} = 1.5$. The curve for $m = 0$ is equivalent to curve A in Figure 2.

quality will not have large effects on the net adhesion force between particles. Of course if the surface concentration is reduced too far (curve E), the repulsive force is not sufficient to overcome the attractive dispersion forces.

The effect of solvent quality for a binary solvent (with the second solvent being a short chain alcohol, such as methanol) is also shown in Figure 3 for Eq. 8 added to Eq. 10. The parameters used here are $\chi_{13} = 0.3$ (as previously), $\chi_{12} = 0.8$ (estimated for octane-methanol), and $\chi_{23} = 1.5$ (estimated for methanol-polyethylene). The other parameters are the same as those for Figure 2 curve A. Figure 3 shows that for moderate levels of the addition of poor solvent, the change in the net attractive force at the interaction potential minimum is small assuming that the presence of the second solvent does not affect adsorption. However, even if the presence of the poorer solvent increases the adsorbed amount of surfactant, this would not significantly affect the net attractive force. The second solvent may also affect the water droplet diameter in emulsions prior to hydrate formation. We have assumed no change in particle size.

The models discussed previously for steric repulsion are fairly simplistic, but they do give an idea as to how various parameters affect the interactions between particles and what is necessary to prevent the particles from coming into contact. For all of these examples, even those where contact between the particles themselves is prevented, there exists a net attractive force between particles. A 2-nm thick steric barrier would not be sufficient to prevent flocculation except for very small particles. An attractive force (F_s/a) of about 2.6×10^{-5} N/m would exist at a particle separation of 4 nm. Next, we will compare steric repulsion with capillary forces, examine the ways that surfactants can affect capillary forces, and then we will examine the strength of these forces relative to shear forces in flow.

Capillary forces

Figure 4 shows capillary adhesion force as a function of subcooling for various values of h using Eqs. 13 to 16 (with $\theta_p = 0^\circ$ and $\sigma = 35$ mN/m). These are compared with the force calculated from Eq. 12 for $h = 0$ and for relatively small subcoolings. A value for a of 250 μm was chosen to compare with hydrate particle adhesion studies.[5] The interfacial tension used is for the system in reference 5 (mixtures of THF with water and decane). F_s/a values in Figure 4 are of similar magnitude compared with those in adhesion studies.[4,6] Note that these values are approximately four-orders of magnitude larger than attractive forces arising from dispersion forces with particles separated by 2 nm steric layers (see above). As mentioned before, the measured adhesion force has been found to decrease as subcooling increases, and this would not be expected for perfect spheres at contact (see Figure 4) if temperature effects on σ and θ_p are neglected. However, surface roughness (small asperities) could give rise to an effective separation between particles, and as shown in Figure 4 this could lead to a decrease in adhesion force with increased subcooling. Asperities of only a few nanometers (modeled in Figure 4) could give rise to decreases in adhesion force comparable to results in references 3 and 5. Further discussion of the effects of surface roughness on capillary forces can be found elsewhere.[4,26,29] The effect of particle size (with constant h) on F_s/a is quite small, and Figure 4 shows that a decrease in a of over two-orders of magnitude leads to only a small change in F_s/a.

AA would be expected to have three possible effects on capillary adhesion. First, the steric layer would separate the particles. Figure 4 shows that an increase from 3 nm to 7 nm in h does lead to a decrease in adhesion force, but this decrease is relatively small especially at small subcoolings. So, this effect alone could not explain the effect of AA. Second, adsorbed surfactant could affect the contact angle of water on the hydrate θ_p. The contact angle through water is given by Young's Equation

$$\cos\theta_p = \frac{\sigma_{ho} - \sigma_{hw}}{\sigma} \tag{19}$$

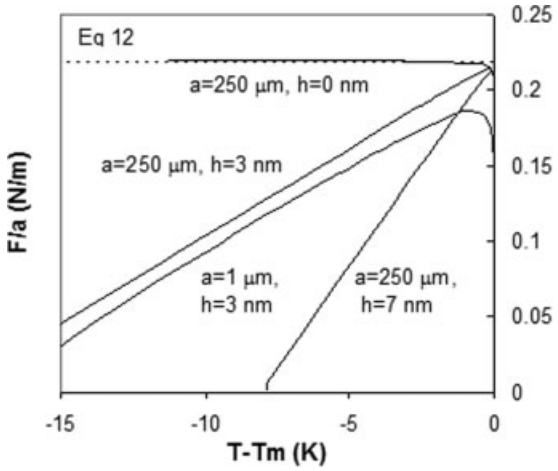

Figure 4. Capillary adhesion force between spheres using Eqs. 13 to 16 (with $\theta_p = 0^\circ$ and $\sigma = 35$ mN/m) showing the effects of particle size and particle separation.

The dotted, temperature-independent line is the result from Eq. 12.

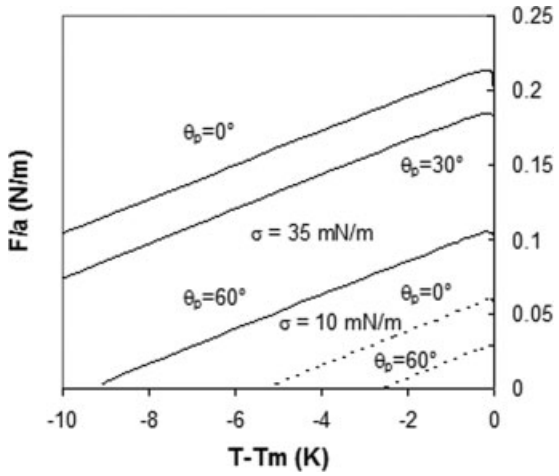

Figure 5. Capillary adhesion force between spheres using Eqs. 13 to 16 (with $a = 250$ μm, and $h = 3$ nm.) showing the effects of contact angle and oil/water interfacial tension.

The solid curves are for $\sigma = 35$ mN/m, while the dotted curves are for $\sigma = 10$ mN/m.

where σ_{ho} is the hydrate-oil interfacial energy, and σ_{hw} is the hydrate-water interfacial energy. For a pure oil (without any surface-active agents) the hydrate surface would be expected to be preferentially wet by the water (small θ_p). Typically, antiagglomerants are either oil soluble or relatively hydrophobic. These types of surfactants may increase the contact angle through water (see for example references 30 and 31) presumably by reducing σ_{ho} in addition to the expected decrease in σ. The σ_{hw} could also be affected. In our experience the use of fluorochemical polymers and its adsorption in rock substrate often increases the contact angle through water from 0° to about 150° by just reducing the surface energies of the substrate, and without affecting the surface tension in the gas-liquid fluid systems.[32] Figure 5 shows how capillary adhesion force is reduced as contact angle is increased between 0° and 60° with $h = 3$ nm. Obviously, once the contact angle reaches a critical value there would be no liquid bridge and no capillary adhesion. Third, surfactant could adsorb at the liquid/liquid interface and lower the interfacial tension. Figure 5 shows how a decrease in interfacial tension from 35 mN/m to 10 mN/m (value arbitrarily chosen) reduces capillary force. For most surfactants the reduction in interfacial tension is orders of magnitude which could lead to a significant reduction in capillary forces. Figure 5 also shows the effect of a combination of interfacial tension decrease and contact angle increase. An additional point to note is that a reduction in interfacial tension and an increase in contact angle not only decrease the attractive force, but the range of temperatures over which a liquid bridge can form is reduced. For $\sigma = 10$ mN/m and $\theta_p = 60°$, the liquid bridge could only exist down to approximately a subcooling of 2–3°C for $h = 3$ nm.

It should be noted that attractive capillary forces at small subcoolings still exist for the cases shown in Figure 5, and these values are far greater than dispersion forces alone, as expected. In addition, the presence of liquid bridges between particles may give rise to particles fusing together as subcooling increases.[6] Thus, it may be necessary for AA to completely prevent capillary adhesion and not just reduce to the adhesion force. In order to completely prevent capillary adhesion, the contact angle must be increased beyond the critical value. In the next section we will compare the adhesion forces to forces experienced during flow.

Shear forces

The magnitude of shear forces from Eq. 17 can be compared to the magnitudes of dispersion and capillary forces. As an estimate, we assume that near the pipe walls, the fluid could experience shear rates at least on the order of 1 s^{-1}. For dispersion forces with $h = 4$ nm, $\mu = 10^{-3}$ Pa·s, and $\gamma = 1$ s^{-1}, Eq. 18 shows that pairs of particles of radius about 1 mm or greater should be broken apart by the shear forces from the relatively small shear rate. This means that although some smaller particles may flocculate together, particles or flocs of about visible size should be broken apart by shear so long as a steric barrier is present to give a particle separation of about 4 nm.

For particles being held by capillary adhesion, if F_s/a for attraction is 0.2 N/m, the minimum particle size for shear forces to break apart a pair is approximately 10 m! Clearly, for a 12″ pipe, the hydrate particle aggregates would be too strong for shear forces. Even if the adhesive force is reduced by an order of magnitude (comparable to what is seen in Figure 5 for a combination of moderate contact angle increase and surface tension reduction at low-subcoolings) the minimum particle size is only reduced an order of magnitude to about 1 m. Again, shear forces could not be expected to break apart particle pairs or even flocs. Thus, it would appear near complete prevention of capillary adhesion would be required to provide sufficient stability for the hydrate particles.

Hydrate Particle Dispersal and Wettability

The discussion earlier reveals that particle size can have an influence on the forces between particles. Particle size will be determined by the conditions before and during hydrate formation. Kelland[10] suggests that there are two ways by which AA act to disperse hydrate particles. If hydrates are confined to the aqueous phase (or the interface of the aqueous phase), then most likely the size of the water droplet will determine the hydrate particle size if all hydrate formed within the droplet eventually fuses together (although some work on ice suggests that certain surfactants may hinder this process[33]). Droplet size would depend on fluid dynamics within the pipe and surface active materials (either added or natural to the oil) that could lower the interfacial tension and stabilize the droplets against coalescence. The presence of AA could lead to smaller droplets, and, thus, smaller hydrate particles.

The other method by which small particles could be formed arises from changes in interfacial tensions (or interfacial energies) from adsorbing surfactant. Due to mass-transfer limitations, hydrate formation takes place at or near the water/oil or water/gas interface. Hoiland et al.[14] discuss how the three interfacial tensions (hydrate/oil, hydrate/water, and oil/water) affect wettability and the position and shape of a hydrate lens at the interface. They show wetting diagrams

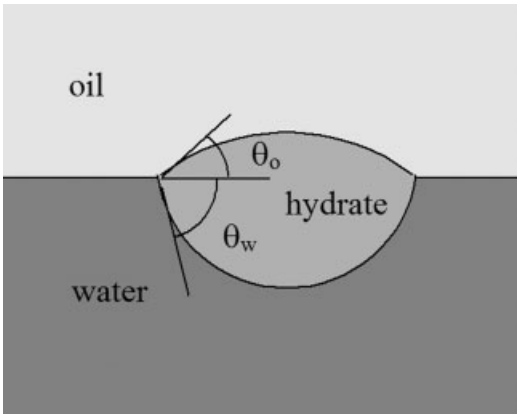

Figure 6. Hydrate lens at an oil-water interface.

indicating the ranges of tensions that allow for a lens to reside at the interface (Figure 6). A similar wetting diagram is shown in Figure 7 for an interfacial tension of 35 mN/m. The wetting diagram is a plot of σ_{ho} vs. σ_{hw}, and shows the ranges of valid interfacial energies such that the particle could reside at the interface. If the energies are such that the upper left boundary ($\theta_o = 0^\circ$) is crossed, then one would have a particle that resides entirely in the aqueous phase. Likewise, if the lower right boundary ($\theta_o = 180^\circ$) is crossed, one would have a particle that resides entirely in the oil phase. The curves are isolines of constant θ_o.

If the hydrate particle is assumed to be a sphere rather than a lens, then a similar wetting diagram can be constructed as shown in Figure 8a, which is a graphical representation of Young's equation (Eq. 19) where the isolines are for constant contact angle through the aqueous phase. A decrease in oil/water interfacial tension causes the boundaries

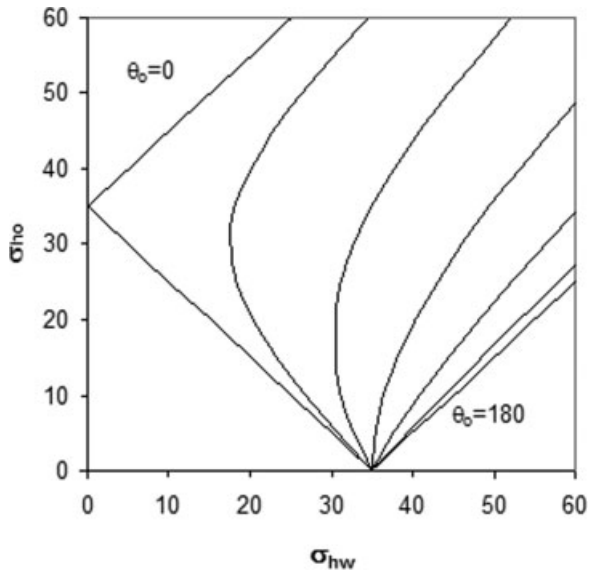

Figure 7. Wetting diagram for a hydrate lens at the oil/water interface for σ = 35 mN/m.

The upper left region would be for a water-wet hydrate particles while the lower right would be for an oil-wet hydrate particle. The isolines are for constant values of θ_o.

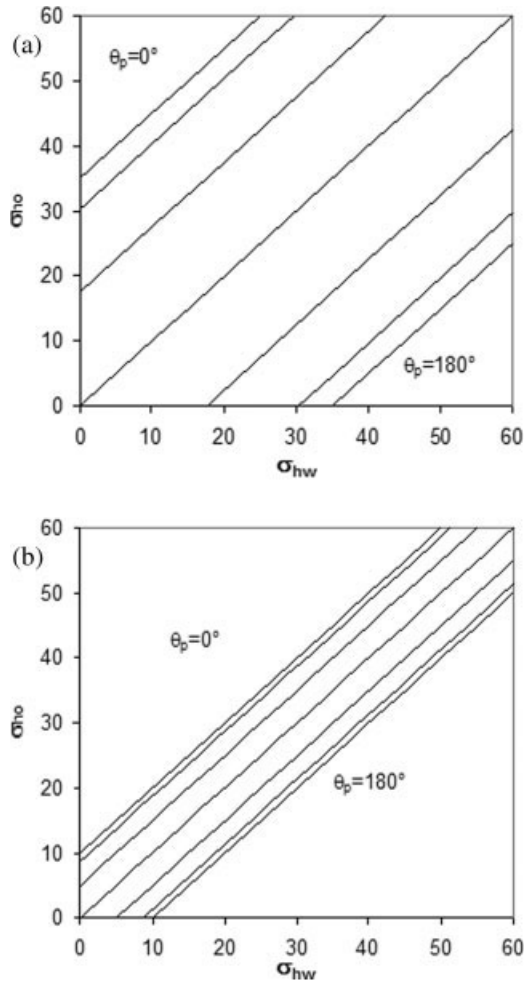

Figure 8. Wetting diagrams for a hydrate sphere at the oil/water interface for (a) σ = 35 mN/m, and (b) σ = 10 mN/m.

of the valid region to move inwards (Figure 8b). A decrease in σ combined with a decrease in oil/hydrate interfacial energy could not only increase the contact angle, but if substantial enough could mean that it would be energetically more favorable for a hydrate particle to exist in the oil phase rather than at the interface or in the aqueous phase. Thus, the hydrate particle could be forced from the interface into the oil phase. Once in the oil phase, the growth rate of the hydrate particle would be reduced greatly owing to the limited supply of water

Conclusions

We draw the following conclusions from this work.

(1) Forces between hydrate particles (by capillary adhesion and solid/solid adhesion) are orders of magnitude larger than what would be expected if the particles were separated by a few nanometers with attraction due to dispersion forces alone.

(2) If particles are held together by dispersion forces alone and if the particles are separated by a steric barrier of a few

nanometers, then shear forces under typical flow conditions should be sufficient to break apart flocs of particles.

(3) AA would most likely need to prevent capillary adhesion by sufficiently reducing interfacial tension and increasing contact angle; even reduced capillary adhesion forces may be strong enough to prevent shear forces from separating the particles, unless there is a very large decrease in interfacial tension or very large shear rates are experienced.

(4) AA should result in small water droplet formation leading to formation of small hydrate particles. This would greatly aid in preventing agglomeration and pipe blockages since the forces between particles would be reduced. However, AA must also provide steric repulsion to reduce the net attraction between particles.

(5) A second solvent, such as methanol does not seem to affect the net adhesive force (steric plus dispersion forces), so long as the adsorbed amount of surfactant and the particle size do not change.

Acknowledgments

This work was supported by the member companies of the Reservoir Engineering Research Institute (RERI) whose support is greatly appreciated.

Literature Cited

1. Anklam MR, Firoozabadi A. An interfacial energy mechanism for the complete inhibition of crystal growth by inhibition adsorption. *J of Chem Phys*. 2005;123,144708–12.
2. Lund A, Larsen R. Conversion of water to hydrate particles - theory and application. Paper presented at: 14th Symposium on Thermophysical Properties; 2000; Boulder, CO.
3. Gudmundsson JS. Cold flow hydrate technology. Proc 4th Int Conf on Gas Hydrates, Yokohama, Japan; 2002;912.
4. Yang S, Kleehammer DM, Huo Z, Sloan ED, Miller KT. Temperature dependence of particle-particle adherence forces in ice and clathrate hydrates. *J Colloid Interface Sci*. 2004;277:335–341.
5. Yang S, Kleehammer DM, Huo Z, Sloan ED, Miller KT. Micromechanical measurements of hydrate particle attractive forces. Paper presented at: 15th Symposium on Thermophysical Properties; 2003; Boulder; CO.
6. Taylor CJ, Dieker LE, Miller KT, Koh CA, Sloan ED. Micromechanical adhesion force measurements between tetrahydrofuran hydrate particles. *J Colloid Interface Sci*. 2007;306:255–261.
7. Derjaguin BV, Muller VM, Toporov YP. Effect of contact deformations on the adhesion of particles. *J Colloid Interface Sci*. 1975; 53:314–326.
8. Johnson KL, Kendall K, Roberts AD. Surface energy and the contact of elastic solids. *Proc R Soc Lond A*. 1971;324:301–313.
9. Camargo R, Palermo T. Rheological properties of hydrate suspensions in an asphaltenic crude oil. Proc 4th Int Conf on Gas Hydrates, Yokohama, Japan; 2002;880.
10. Kelland MA. History of the development of low dosage hydrate inhibitors. *Energy & Fuels*. 2006;20:825–847.
11. Free ML, Shah DO. Enhancement of particle removal and modification of interfacial phenomena using surfactants. In: Mittal KL. *Particles on Surfaces 7: Detection, Adhesion, and Removal*. Boston: VSP; 2002:405–418.
12. Zelenev A, Matijevic E. Surfactant-induced detachment of monodispersed hematite particles adhered on glass. *J Colloid Interface Sci*. 2006;299:22–27.
13. Huo Z, Freer E, Lamar M, Sannigrahi B, Knauss DM, Sloan ED. Hydrate plug prevention by anti-agglomeration. *Chem Eng Sci*. 2001;56:4979–4991.
14. Hoiland S, Borgund AE, Barth T, Fotland P, Askvik KM. Wettability of Freon hydrates in crude oil/brine emulsions: the effects of chemical additives. Proc 5th Int Conf on Gas Hydrates, Trondheim, Norway; 2005.
15. Zanota ML, Dicharry C, Graciaa A. Hydrate plug prevention by quaternary ammonium salts. *Energy & Fuels*. 2005;19:584–590.
16. Fleer GJ, Cohen Stuart MA, Scheutjens JMHM, Cosgrove T, Vincent B. *Polymers at Interfaces*. London: Chapman & Hall; 1998.
17. Hiemenz PC, Rajagopalan R. *Principles of Colloid and Surface Chemistry*. (3rd ed). New York: Marcel Dekker; 1997.
18. Napper DH. *Polymeric Stabilization of Colloidal Dispersions*. London: Academic Press; 1983.
19. Everett DH, *Faraday Disc Chem Soc*. 1978;65:215–229.
20. Derjaguin BV. Friction and adhesion. IV. The theory of adhesion of small particles. *Kolloid-Z*. 1934;69:155–164.
21. Pouchly J, Zivny A, Solc K. Thermodynamic equilibrium in the system macromolecular coil binary solvent. *J Polym Sci, Part C*. 1968;23:245–256.
22. Young TH, Cheng LP, Hsieh CC, Chen LW. Phase behavior of EVAL polymers in water-2-propanol cosolvent. *Macromolecules*. 1998;31:1229–1235.
23. Russel WB, Saville DA, Schowalter WR. *Colloidal Dispersions*. Cambridge: Cambridge University Press; 1989.
24. Israelachvili JN. *Intermolecular and Surface Forces*. (2nd ed). San Diego: Academic Press, 1992.
25. Jones R, Pollack HM, Cleaver JAS, Hodges CS. Adhesion forces between glass and silicon surfaces in air studied by AFM: effects of relative humidity, particle size, roughness, and surface treatment. *Langmuir*. 2002;18:8045–8055.
26. Rabinovich YI, Adler JJ, Esayanur MS, Ata A, Singh RK, Moudgil BM. Capillary forces between surfaces with nanoscale roughness. *Adv Colloid Interface Sci*. 2002;96:213–230.
27. Biggs S, Cain RG, Dagastine RR, Page NW. Direct measurements of the adhesion between a glass particle and a glass surface in a humid atmosphere. *J Adhes Sci Technol*. 2002;16:869–885.
28. de Lazzer A, Dreyer M, Rath HJ. Particle-surface capillary forces. *Langmuir*. 1999;15:4551–4559.
29. Ata A, Rabinovich YI, Singh RK. Role of surface roughness in capillary adhesion. *J Adhes Sci Technol*. 2002;16:337–346.
30. Bryant EM, Bowman RS, Buckley JS. Wetting alteration of mica surfaces with polyethoxylated amine surfactants. *J Pet Sci Eng*. 2006;52:244–252.
31. Skalli L, Buckley JS, Zhang Y, Morrow NR. Surface and core wetting effects of surfactants in oil-based drilling fluids. *J Pet Sci Eng*. 2006;52:253–260.
32. Fahes M, Firoozabadi A. Wettability alteration to intermediate gas-wetting in gas-condensate reservoirs at high temperatures. *SPE J* 2007;12:397–407.
33. Kitamoto D, Yanagishita H, Endo A, Nakaiwa M, Nakane T, Akiya T. Remarkable antiagglomeration effect of a yeast biosurfactant, diacylmannosylerythritol, on ice-water slurry for cold thermal storage. *Biotechnol Prog*. 2001;17:362–365.

Appendix

Derivation of Everett's theory for steric repulsion and extension to ternary systems

In this theory developed by Everett,[17,18] the change in free energy is computed vs distance for two parallel plates with adsorbed polymer or surfactant. The concentration of chains is assumed uniform between the plates, and all chains between the plates are assumed to be adsorbed. Free energy is calculated using Flory-Huggins theory. The force per unit area acting on the plates separated by a distance h to keep the system at equilibrium (i.e., the repulsive force) can be written as

$$f - f_0 = \int_0^{n_2} -\frac{1}{A_p}\left(\frac{\partial \mu_2}{\partial h}\right)_{n_2} dn_2 \qquad \text{(A1)}$$

where A_p is the area of each plate, μ_2 is the chemical potential of the polymer/surfactant, and n_2 is the number of molecules of polymer/surfactant between the plates. Using Flory-Huggins theory neglecting translational entropy (assuming fixed ends

on the chains) and assuming $r \gg 1$ the force between plates is given by

$$f - f_0 = kT\left[\frac{4\Gamma^2 v_2 r^2}{h^2}(1/2 - \chi_{12}) + \frac{16\Gamma^3\, r^3 v_2^2 \chi_{12}}{h^3}\right] \quad \text{(A2)}$$

where the surface concentration is now given by

$$\Gamma = \frac{n_2}{2A_p} \quad \text{(A3)}$$

This force can be converted to a potential (per unit area) between plates using

$$\Phi(\Gamma, h) - \Phi(0, h) = \Phi(h) = -\int_{\infty}^{h} (f - f_0)dh \quad \text{(A4)}$$

Assuming that the potential is zero at $h = 2\delta$, the potential at any separation less than 2δ is

$$\Phi(h) = kT\left[4\Gamma^2 v_2 r^2\left(\frac{1}{h} - \frac{1}{2\delta}\right)(1/2 - \chi_{12}) + (8/3)\Gamma^3 r^3 v_2^2 \chi_{12}\left(\frac{1}{h^2} - \frac{1}{4\delta^2}\right)\right]$$

$$h \le 2\delta \quad \text{(A5)}$$

This potential between flat plates can be used to calculate the force or potential between spheres using the Derjaguin approximation.[18]

$$\Phi_s \approx \pi a \int_{h}^{2\delta} \Phi(h)dh = \pi akT\left[\begin{array}{l} 4\Gamma^2 v_2 r^2\left(\ln\left(\frac{2\delta}{h}\right) - \frac{2\delta - h}{2\delta}\right)(1/2 - \chi_{12}) \\ + (8/3)\Gamma^3 r^3 v_2^2 \chi_{12}\left(\frac{1}{h} - \frac{1}{2\delta} - \frac{2\delta - h}{4\delta^2}\right) \end{array}\right] \quad \text{(A6)}$$

where h is now the minimum distance between spheres. The aforementioned expression is the same as Eq. 5.

For a ternary system, the force (per area) between plates can be written as

$$f - f_0 = \int_{0}^{n_3} -\frac{1}{A_p}\left(\frac{\partial \mu_3}{\partial h}\right)_{n_2} dn_3 \quad \text{(A7)}$$

Using Eqs. 14 and 16 and the definition of chemical potential and neglecting the translational entropy term for species 3 we find for $r \gg 1$

$$f - f_0 = kT\left[\begin{array}{l} \frac{4\Gamma^2 r^2 v_3}{h^2}\left(\frac{1}{2} - \frac{\chi_{13}}{1+m} - \frac{\chi_{23} m}{1+m} + \frac{\chi_{12} m}{(1+m)^2}\right) \\ + \frac{16\Gamma^3 r^3 v_3^4}{3h^3}\left(\frac{\chi_{13}}{1+m} + \frac{\chi_{23} m}{1+m} - \frac{\chi_{12} m}{(1+m)^2}\right) \end{array}\right] \quad \text{(A8)}$$

Using the Derjaguin approximation (Eqs. 9 and 12) the force between spheres is found to be

$$F_S = \pi akT \times \left[\begin{array}{l} 4\Gamma^2 r^2 v_3\left(\frac{1}{h} - \frac{1}{2\delta}\right)\left(\frac{1}{2} - \frac{\chi_{13}}{1+m} - \frac{\chi_{23} m}{1+m} + \frac{\chi_{12} m}{(1+m)^2}\right) \\ + (8/3)\Gamma^3 r^3 v_3^4\left(\frac{1}{h^2} - \frac{1}{4\delta^2}\right)\left(\frac{\chi_{13}}{1+m} + \frac{\chi_{23} m}{1+m} - \frac{\chi_{12} m}{(1+m)^2}\right) \end{array}\right] \quad \text{(A9)}$$

which is the same as Eq. 9.

Manuscript received Aug. 9, 2007.